

# PROBING HALO AND MOLECULAR STATES IN LIGHT, NEUTRON-RICH NUCLEI

N.A. ORR

*LPC-ISMRA, Bd Maréchal Juin, 14050 Caen Cedex, France*

*e-mail: orr@caelav.in2p3.fr*

Selected topics on halo and molecular states in light, neutron-rich nuclei are discussed. In particular, work on  $x\alpha:Xn$  structures is briefly reviewed. The use of proton radiative capture as a probe of clustering is also presented through the example provided by the  ${}^6\text{He}(p,\gamma)$  reaction.

## 1 Introduction

Until relatively recently cluster studies have been confined to the region encompassing the line of beta stability. As clustering is expected to manifest itself most strongly near thresholds<sup>1</sup>, exotic structures might be expected to form in the more weakly bound systems found in the vicinity of the driplines. Perhaps the most striking example of this are the halo nuclei.

In the present paper two topics are addressed. Firstly a brief review is given of the status of work on  $x\alpha:Xn$  molecular states. Secondly radiative capture of protons is investigated as a probe of clustering through the example provided by the reaction  ${}^6\text{He}(p,\gamma)$  at 40 MeV.

## 2 Molecular States

Owing to the strongly bound character of the  ${}^4\text{He}$  nucleus and the weakness of the  $\alpha$ - $\alpha$  interaction the  $\alpha$ -particle plays an important rôle in the structure of light  $\alpha$ -conjugate nuclei. Whilst an excess of neutrons (or protons) might naively be expected to dilute any underlying  $\alpha$ -cluster structures, theoretical<sup>2,3</sup> and recent experimental work<sup>4,5</sup> indicate that molecular-type structures such as  $\alpha$ -chains “bound” by valence nucleons also occur. The appearance of such cluster structures is well illustrated, as discussed here, by the beryllium isotopes, for which the  $\alpha$ - $\alpha$  system may be regarded as the basis.

As described at this symposium a variety of theoretical models exist. For example, the Molecular-Orbital Model (MO)<sup>2</sup>, in which valence nucleons are added to the single-particle orbits arising from the two-centre potential, provides a conceptually appealing framework within which to describe the properties of these nuclei. Moreover these orbits may be interpreted as the analogues of the  $\sigma$  and  $\pi$ -orbitals associated with the covalent binding of

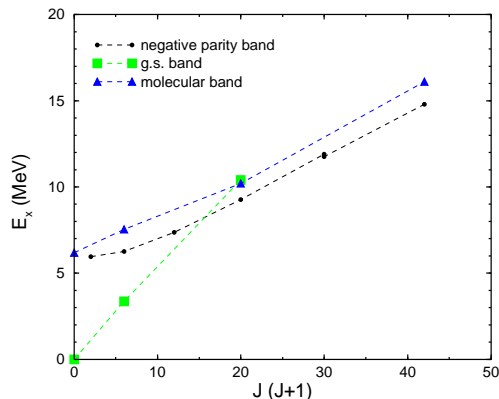


Figure 1. Spin-energy systematics for states observed in  $^{10}\text{Be}$  (from ref.<sup>7</sup>). The trajectories of the postulated positive and negative parity molecular bands are indicated.

atomic molecules. The development of fully fledged Antisymmetrised Molecular Dynamics calculations (AMD), as discussed by Kanada En'yo in her contribution to YKIS01, is of particular interest as the nucleus is modelled without any a priori imposition of an underlying cluster structure.

From an experimental perspective systematic evidence for the existence of dimers in  $^{9-11}\text{Be}$  and  $^{9-11}\text{B}$  has been compiled<sup>4</sup>. In the case of  $^9\text{Be}$ , for example, many facets of the level structure may be understood in terms of a three-body  $\alpha:n:\alpha$  molecular structure. In particular, the rotational bands based on the ground and low-lying states exhibit large deformations consistent with the associated molecular configurations.

In the case of  $^{10}\text{Be}$ , the experimental evidence for molecular configurations is rather less well documented. Beyond the established  $0_2^+$ ,  $2_2^+$  and  $1_1^- - 4_1^-$  states, the locations of the  $J=5^+$  and  $6^-$  members of the negative parity band, as well as the  $J=4^+$  and  $6^-$  members of the positive parity band have been postulated following studies of the  $\alpha$ - $^6\text{He}$  breakup of  $^{10}\text{Be}$ \*<sup>6,7</sup>. Recently, Curtis *et al.* have succeeded in determining the spins of the levels at 9.56 (J=2) and 10.15 MeV (J=3)<sup>8</sup>. As displayed in Fig. 1, the spin-energy trajectories for the bands based on the  $0_2^+$  and  $1_1^-$  states at  $\sim 6$  MeV are consistent with large deformations ( $\hbar^2/2\mathcal{I} \simeq 0.23$  MeV) as expected for molecular-like  $\alpha:2n:\alpha$  structures. Theoretical support may be found in AMD calculations, whereby well developed  $\alpha:2n:\alpha$  configurations are predicted for the  $0_2^+$  and  $1_1^-$  bands<sup>3</sup>. Furthermore, in extended MO model calculations the  $0_2^+$  state appears to be well characterised by valence neutrons occupying the  $\sigma$ -orbital<sup>9</sup>.

Given the existence of such molecular-type structures in  $^{10}\text{Be}$ , the ques-

tion naturally arises as to the existence of similar structures in more neutron-rich systems. In this context we investigated the dripline nucleus  $^{12}\text{Be}$  via inelastic scattering at 35 MeV/nucleon. Evidence was found in these measurements for the breakup into  $^6\text{He}+^6\text{He}$  and  $\alpha+^8\text{He}$  of states (J=4, 6, 8) in the range  $E_x=10\text{-}20$  MeV which exhibit spin-energy systematics characteristic of a rotational band<sup>5,7</sup>. Moreover the inferred momenta of inertia –  $\hbar^2/2\mathfrak{I}=0.15\pm 0.04$  MeV – and bandhead energy (10.8 $\pm$ 1.8 MeV) are consistent with the cluster decay of a molecular structure which may be associated with  $\alpha;4n:\alpha$  configurations. As reported at this symposium by Saito, an experiment using two neutron removal from an energetic  $^{14}\text{Be}$  beam has recently uncovered a probable  $0^+$  state some 1.7 MeV ( $E_x=11.8$  MeV) above the  $^6\text{He}+^6\text{He}$  breakup threshold, as well as weaker evidence for the levels observed in our work. The location of this new level conforms reasonably well to the spin-energy systematics established in our original study and suggests, interestingly, that the bandhead lies above the  $^6\text{He}+^6\text{He}$  threshold.

The theoretical investigation of molecular configurations in  $^{12}\text{Be}$  represents a more challenging venture than the lighter mass Be isotopes. Nevertheless, efforts are underway, as evidenced by the contribution of Ito to this symposium and recent papers by Itagaki *et al.*<sup>9</sup> and Descouvemont and Baye<sup>10</sup>.

As suggested by von Oertzen<sup>4</sup> and more recently by Itagaki *et al.*<sup>11</sup>, the neutron-rich C isotopes may be expected to exhibit  $3\alpha:\text{Xn}$  cluster structures. In this context, we have attempted to observe such states in the  $^{12}\text{C}(^{16}\text{C}, ^{16}\text{C}^* \rightarrow ^{10,12}\text{Be}^* + ^{6,4}\text{He})$  reaction at 35 MeV/nucleon<sup>12</sup>. Careful analysis of the associated  $^6\text{He}+^6\text{He}+\alpha$  and  $^8\text{He}+2\alpha$  fragment coincidences could, however, only put an upper limit of some  $2\mu\text{b}$  on the yield to states in these decay channels<sup>a</sup>. The inability to access such states by inelastic scattering may arise from a much smaller overlap between the  $^{16}\text{C}$  ground state and the cluster states than in the case of  $^{12}\text{Be}$ .

### 3 Radiative proton capture on $^6\text{He}$

A recent investigation of coherent bremsstrahlung production in the reaction  $\alpha(p,\gamma)$  at 50 MeV has demonstrated, as described in the accompanying contribution by Herbert Loehner, that the high-energy photon spectrum is dominated by capture to form  $^5\text{Li}$ <sup>13</sup>. This result motivated us to extend the technique to probe clustering in more exotic systems<sup>14</sup>. As a first test  $^6\text{He}$  was chosen owing to the relatively high beam intensities available and the fact that

<sup>a</sup>An upper limit of  $30\mu\text{b}$  could be put on the  $^{10,12}\text{Be}_{gs}+^{6,4}\text{He}$  decay channels.

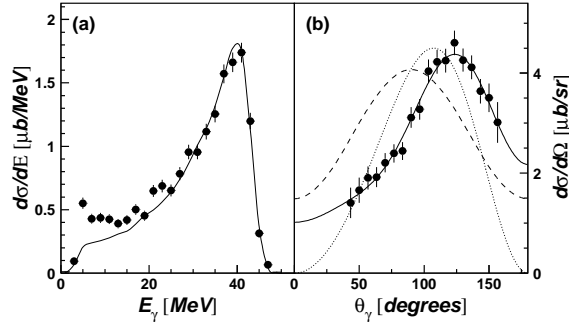


Figure 2. Energy (a) and angular distributions (b) in the  ${}^6\text{He}+p$  c.m. for photons in coincidence with  ${}^7\text{Li}$ . The solid line in (a) is the response of the Chateau to  $E_\gamma = 42$  MeV. The lines in (b) are a classical electrodynamics calculation<sup>15</sup> (dotted), a cluster model<sup>14,16</sup> (dashed), both normalized to the data, and a Legendre polynomial fit<sup>17</sup> (solid).

structurally it is the most well established two-neutron halo nucleus. Given a proton wavelength of 0.7 fm at 40 MeV, direct capture might be observed, as a quasi-free process, on the constituents ( $\alpha+n+n$ ) of  ${}^6\text{He}$  in addition to capture into  ${}^7\text{Li}$ . Moreover, the different quasi-free capture (QFC) processes would lead to different  $E_\gamma$  in the range 20–40 MeV.

Experimentally, a 40 MeV/nucleon  ${}^6\text{He}$  beam ( $5 \times 10^5$  pps) was employed to bombard a solid hydrogen target ( $95 \text{ mg/cm}^2$ ). The different charged reaction products were identified and momentum analysed using the SPEG spectrometer. The photons were detected using 74 elements of the “Chateau de Cristal”  $\text{BaF}_2$  array, with a total efficiency of some 70%. Further details including the analysis techniques may be found in ref.<sup>14</sup>.

Turning to the experimental observations, the reaction  ${}^6\text{He}(p,\gamma){}^7\text{Li}$  is unambiguously identified by the  $\gamma$ -rays in coincidence with  ${}^7\text{Li}$  (Fig. 2). In particular, the photon energy spectrum, as well as the  ${}^7\text{Li}$  momentum<sup>14</sup>, is well described assuming a  $\gamma$ -ray line at 42 MeV. The energy difference between the two particle-stable states of  ${}^7\text{Li}$  – the g.s. and the first excited state at 0.48 MeV – is too small for them to be distinguished in this experiment. A total cross section of  $\sigma = 35 \pm 2 \mu\text{b}$  was deduced.

The  ${}^6\text{He}(p,\gamma){}^7\text{Li}$  cross section has been calculated using a microscopic cluster model<sup>16</sup>. At 40 MeV, a cross section of  $\sigma = 59 \mu\text{b}$  was found, with  $15 \mu\text{b}$  going to the g.s. and  $44 \mu\text{b}$  to the first excited state<sup>14</sup>. The calculation was restricted to the dominant E1 multipolarity, thus leading to an angular distribution symmetric about  $90^\circ$  (Fig. 2b). The cross section to the g.s. can also be estimated from photodisintegration measurements<sup>18</sup> via detailed

balance considerations and is  $9.6 \pm 0.4 \mu\text{b}$ . Given the predicted relative populations of the ground and first excited state, a total capture cross section of  $\sigma \sim 38 \mu\text{b}$  is obtained, in agreement with the value measured here.

QFC was investigated by searching for  $\gamma$ -rays in coincidence with fragments lighter than  ${}^7\text{Li}$ . The corresponding energy spectra (Fig. 3a,c,e) do indeed exhibit peaks below 42 MeV. In order to establish the origin of these fragment- $\gamma$  coincidences, QFC processes on the subsystems of  ${}^6\text{He}$  have been modelled as follows. The  ${}^6\text{He}$  projectile was considered as a cluster ( $A$ ) plus spectator ( $a$ ) system in which each component has an intrinsic momentum distribution, the corresponding energy  $E_A + E_a - m_{{}^6\text{He}}$  being taken into account in the total available energy. The reaction may be denoted as  $a+A(p,\gamma)B+a$ , and the  $\gamma$ -ray angular distribution is assumed to be that given by the charge asymmetry of the entrance channel<sup>15</sup>. The intrinsic momentum distribution of all the clusters was taken to be Gaussian in form (FWHM = 80 MeV/ $c$ ). In order to explore the possibility that FSI may occur in the exit channel between the spectator,  $a$ , and the capture fragment,  $B$ , an extended version of the QFC calculation was developed<sup>14</sup>. Here the energy in the system  $B+a$  is treated as an excitation in the continuum of  ${}^7\text{Li}$ , which decays in flight.

In the case of  ${}^6\text{Li}$ - $\gamma$  coincidences, two lines were observed (Fig. 3a) at 30 and 3.56 MeV corresponding to the formation of  ${}^6\text{Li}$  and the decay of the second excited state. It was estimated that  ${}^6\text{Li}$  is formed almost exclusively ( $96_{-24}^{+4}\%$ ) in the 3.56 MeV excited state. The deduced cross section was  $\sigma = 3.5 \pm 1.3 \mu\text{b}$ . The lines in Fig. 3a,b corresponds to QFC on  ${}^5\text{He}$  into  ${}^6\text{Li}^*$  (3.56 MeV). The  $\gamma$ -ray energy spectrum is well described, whilst the  ${}^6\text{Li}$  momentum distribution requires inclusion of  ${}^6\text{Li}$ -n FSI.

Evidence for QFC on the  $\alpha$  core, whereby the two halo neutrons would behave as spectators, has also been searched for. The photon spectrum should resemble that observed for the  $\alpha+p$  reaction<sup>13</sup>. Indeed such a  $\gamma$ -ray energy spectrum (Fig. 3c) was observed. The background, however, arising from  ${}^6\text{He}$  breakup, in which the  $\alpha$  particle is detected in SPEG and the halo neutrons interact with the forward-angle detectors of the Château, is significant. In order to minimise this background, only the backward-angle detectors ( $\theta > 110^\circ$ ) of the Château were used in the analysis. The  $\gamma$ -ray spectrum under this condition exhibits two components: a peak at  $E_\gamma = 27$  MeV and a  $1/E_\gamma$  continuum similar to coherent  $\alpha+p$  bremsstrahlung<sup>13</sup>.

Simulations indicate, however, that some back-scattered neutrons remain from breakup, which would also lead to a continuous component with a  $1/E$  type spectrum in the Château<sup>14</sup>. A single background component of this form (dotted line, Fig. 3c) was therefore added to the QFC process  $\alpha(p,\gamma){}^5\text{Li}$ . The photon energy spectrum is thus well described, as is the momentum

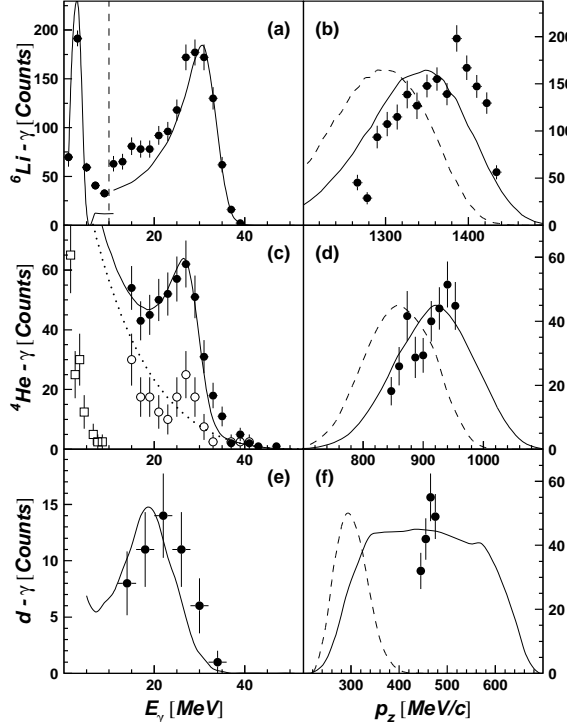


Figure 3. Gamma-ray energy spectrum in the  ${}^6\text{He}+p$  c.m. and momentum distribution of the coincident fragment for  ${}^6\text{Li}$  (upper),  $\alpha$  particles (middle) and deuterons (lower panel). The lines correspond to calculations of QFC on the  ${}^5\text{He}$  cluster, the  $\alpha$  core and one halo neutron, respectively, on the right with/without (solid/dashed) fragment FSI (see text). The distribution in (a) was divided by 3 below 10 MeV, and the open symbols in (c) are from an analysis investigating the role of the neutron background (see ref.<sup>14</sup>).

distribution of the  $\alpha$  particle. The cross section was estimated to be  $\sigma = 4 \pm 1 \mu\text{b}$ . Additional support for this interpretation is found in  $\alpha$ - $\gamma$ -n coincidences, for which 30 events were observed<sup>14</sup> (open symbols, Fig. 3c).

Finally, d- $\gamma$  coincidences presenting a peak in the  $\gamma$ -ray energy spectrum, at  $E_\gamma \simeq 21$  MeV, were also observed (Fig. 3e). The relatively low statistics arose from the limited acceptances of the spectrometer for deuterons (Fig. 3f). The predictions for  $n(p,\gamma)d$  QFC on a halo neutron present a peak at 19 MeV (Fig. 3e) – the small shift may be attributable to the strong kinematic correlation between the deuteron momentum and the photon energy, as the detection of only a small fraction of the deuterons is predicted<sup>14</sup>. As such no reliable

estimate of the cross section was possible.

There are additional QFC channels,  $2n(p,\gamma)t$  and  $t(p,\gamma)\alpha$ , that could have been observed with finite efficiency but were not<sup>14</sup>. Perhaps the most interesting is QFC on the two halo neutrons. In the case of  ${}^6\text{He}$ , several theoretical models predict the coexistence of two configurations in the g.s. wave function: the so-called “di-neutron” and “cigar” configurations<sup>19</sup>. Here one might expect that the different admixtures of these could be probed by the relative strength of the  $n, 2n(p,\gamma)d, t$  QFC processes, whereby the corresponding free cross sections at 40 MeV, obtained from detailed balance considerations, are comparable:  $9.6\mu\text{b}$ <sup>20</sup> and  $9.8\mu\text{b}$ <sup>21</sup>, respectively. However, events registered in the Château in coincidence with tritons in SPEG have energies below 10 MeV, whereas the  $2n(p,\gamma)t$  reaction should produce photons with  $E_\gamma \approx 32$  MeV.

As described above, the QFC with fragment FSI model describes well the observed monoenergetic  $\gamma$ -rays, as well as the momentum distribution of the capture fragment ( $B$ ). The  $\gamma$ -ray lines are associated with specific energy distributions for the fragments in the exit channel. Therefore, such a process will exhibit the same kinematics as capture into continuum states above the corresponding threshold,  ${}^6\text{He}(p,\gamma){}^7\text{Li}^* \rightarrow B+a$ , provided that the equivalent region of the continuum is populated<sup>14</sup>. If, however, all the final states observed here were the result of radiative capture into  ${}^7\text{Li}$ , capture via the non-resonant continuum in  ${}^7\text{Li}$  might well be expected to occur<sup>22</sup>. This would lead to a continuous component to the  $\gamma$ -ray energy spectra. Moreover, events corresponding to  $E_{7\text{Li}^*} = 0.5\text{--}10$  MeV have not been observed in either  $t$ - $\gamma$  coincidences or  $\alpha$ - $\gamma$  coincidences with  $E_\gamma = 32\text{--}42$  MeV, nor has the decay into  $\alpha+t$  for  $E_{7\text{Li}^*} > 10$  MeV. Within the picture of QFC on clusters, this is simply explained by the absence of the  $2n(p,\gamma)t$  and  $t(p,\gamma)\alpha$  QFC processes for the  ${}^4\text{He}$ - $2n$  and  $t$ - $t$  configurations, respectively, indicating that  ${}^4\text{He}$ - $n$ - $n$  is the dominant configuration in  ${}^6\text{He}$ . This is in agreement with the a recent neutron-neutron interferometry measurement we have performed ref.<sup>23</sup>.

## 4 Conclusions

An aperçu of  $x\alpha:Xn$  clustering has been presented and some examples from the neutron-rich Be isotopes discussed. In the very near future, transfer reactions using the combination of low-energy radioactive beams such as  ${}^6,8\text{He}$  and targets ( ${}^6,7\text{Li}$ ,  ${}^9\text{Be}$ ,  ${}^{12}\text{C}$ ) presenting  $\alpha$ -clustering will be investigated as a tool to access molecular-type states in neutron-rich nuclei. Additionally, it is hoped that partial decay widths may be determined.

Radiative proton capture has been explored as a probe of clustering in the ground states of nuclei far from stability through the example of a measure-

ment on the halo nucleus  ${}^6\text{He}$ . In addition to  ${}^6\text{He}(p,\gamma){}^7\text{Li}$ , evidence for QFC on  ${}^5\text{He}$ ,  $\alpha$  and  $n$  was found. Of particular importance was the observation of events which correspond to the previously measured  $\alpha(p,\gamma)$  reaction, as well as the non-observation of capture on a di-neutron. Theoretically, models need to be developed to describe capture on the constituent clusters of exotic nuclei and, for comparison, capture on the projectile into unbound final states.

### Acknowledgments

I would like to underline the leading rôles played by Martin Freer (molecular states), Emmanuel Sauvan and Miguel Marqués (radiative capture). It is a pleasure also to thank the members of the E281 and E302 collaborations for their efforts and the SPEG crew for developing the hydrogen target.

### References

1. K. Ikeda, Prog. Theor. Phys. (Japan) Suppl. (1968) 464
2. M. Seya *et al.*, Prog. Theor. Phys. (Japan) **65** (1968) 205
3. Y. Kanada-En'yo *et al.*, Phys. Rev. **C60** (1999) 064304 and refs therein
4. W. von Oertzen, Z. Phys. **A354** (1996) 37; **A357** (1997) 355
5. M. Freer *et al.*, Phys. Rev. Lett. **82** (1999) 1383
6. N. Soić *et al.*, Europhys. Lett. **34** (1996) 7
7. M. Freer *et al.*, Phys. Rev. **C62** (2001) 034301
8. N. Curtis *et al.*, Phys. Rev. **C64** (2001) 044604
9. N. Itagaki *et al.*, Phys. Rev. **C61** (2000) 044306
10. P. Descouvemont, D. Baye, Phys. Lett. **B505** (2001) 71
11. N. Itagaki *et al.*, Phys. Rev. **C64** (2001) 014301
12. P.J. Leask *et al.*, J. Phys. **G27** (2001) B9
13. M. Hoefman *et al.*, Phys. Rev. Lett. **85** (2000) 1404
14. E. Sauvan *et al.*, Phys. Rev. Lett. **87** (2001) 042501  
E. Sauvan, Thèse, Université de Caen, LPCC T-00-01 (2000)
15. M. Hoefman *et al.*, Nucl. Phys. A **654** (1999) 779c
16. P. Descouvemont, Nucl. Phys. A **584** (1995) 532
17. H.R. Weller *et al.*, Phys. Rev. C **25** (1982) 2921
18. M.R. Sené *et al.*, Nucl. Phys. A **442** (1985) 215
19. M.V. Zhukov *et al.*, Phys. Rep. **231** (1993) 151
20. J. Ahrens *et al.*, Phys. Lett. **52B** (1974) 49
21. D.D. Faul *et al.*, Phys. Rev. Lett. **44** (1980) 129
22. S.A. Siddiqui, N. Dytlewski, H.H. Thies, Nucl. Phys. A **458**, 387 (1986)
23. F.M. Marqués *et al.*, Phys. Lett. B **476** (2000) 219